

Comparing Acceleration and Speed Tuning in Macaque MT: Physiology and Modeling

N.S.C. Price, S. Ono, M. J. Mustari and M. R. Ibbotson

J Neurophysiol 94:3451-3464, 2005. First published Aug 3, 2005; doi:10.1152/jn.00564.2005

You might find this additional information useful...

This article cites 28 articles, 13 of which you can access free at:

<http://jn.physiology.org/cgi/content/full/94/5/3451#BIBL>

This article has been cited by 2 other HighWire hosted articles:

Interactions between Speed and Contrast Tuning in the Middle Temporal Area: Implications for the Neural Code for Speed.

B. Krekelberg, R. J. A. van Wezel and T. D. Albright
J. Neurosci., August 30, 2006; 26 (35): 8988-8998.

[\[Abstract\]](#) [\[Full Text\]](#) [\[PDF\]](#)

Neurons in V1, V2, and PMLS of Cat Cortex Are Speed Tuned But Not Acceleration Tuned: The Influence of Motion Adaptation

N.S.C. Price, N. A. Crowder, M. A. Hietanen and M. R. Ibbotson
J Neurophysiol, February 1, 2006; 95 (2): 660-673.

[\[Abstract\]](#) [\[Full Text\]](#) [\[PDF\]](#)

Updated information and services including high-resolution figures, can be found at:

<http://jn.physiology.org/cgi/content/full/94/5/3451>

Additional material and information about *Journal of Neurophysiology* can be found at:

<http://www.the-aps.org/publications/jn>

This information is current as of February 3, 2007 .

Comparing Acceleration and Speed Tuning in Macaque MT: Physiology and Modeling

N.S.C. Price,¹ S. Ono,² M. J. Mustari,^{2,3} and M. R. Ibbotson^{1,2}

¹Visual Sciences, Research School of Biological Sciences, Australian National University, Canberra, Australian Capital Territory, Australia; and

²Visual Sciences, Yerkes National Primate Research Center and ³Department of Neurology, Emory University, Atlanta, Georgia

Submitted 31 May 2005; accepted in final form 2 August 2005

Price, N.S.C., S. Ono, M. J. Mustari, and M. R. Ibbotson. Comparing acceleration and speed tuning in macaque MT: physiology and modeling. *J Neurophysiol* 94: 3451–3464, 2005. First published August 3, 2005; doi:10.1152/jn.00564.2005. Studies of individual neurons in area MT have traditionally investigated their sensitivity to constant speeds. We investigated acceleration sensitivity in MT neurons by comparing their responses to constant steps and linear ramps in stimulus speed. Speed ramps constituted constant accelerations and decelerations between 0 and 240°/s. Our results suggest that MT neurons do not have explicit acceleration sensitivity, although speed changes affected their responses in three main ways. First, accelerations typically evoked higher responses than the corresponding deceleration rate at all rates tested. We show that this can be explained by adaptation mechanisms rather than differential processing of positive and negative speed gradients. Second, we inferred a cell's preferred speed from the responses to speed ramps by finding the stimulus speed at the latency-adjusted time when response amplitude peaked. In most cells, the preferred speeds inferred from deceleration were higher than those for accelerations of the same rate or from steps in stimulus speed. Third, neuron responses to speed ramps were not well predicted by the transient or sustained responses to steps in stimulus speed. Based on these findings, we developed a model incorporating adaptation and a neuron's speed tuning that predicted the higher inferred speeds and lower spike rates for deceleration responses compared with acceleration responses. This model did not predict acceleration-specific responses, in accordance with the lack of acceleration sensitivity in the neurons. The outputs of this single-cell model were passed to a population-vector-based model used to estimate stimulus speed and acceleration. We show that such a model can accurately estimate relative speed and acceleration using information from the population of neurons in area MT.

INTRODUCTION

Visual motion can be described by its direction, position, and speed. Physiological and behavioral studies have demonstrated that primates have neurons sensitive to these parameters, facilitating accurate motion perception and eye movements (Born and Bradley 2005; Lisberger et al. 1987). It is not clear to what extent neurons are sensitive to higher-order temporal derivatives of position such as acceleration, or how acceleration sensitivity may underlie perception and eye movement control.

Limitations in processing acceleration are thought to similarly affect systems controlling eye movements and motion perception (Watamaniuk and Heinen 2003). Humans can detect differences in stimulus speeds of <5% (McKee 1981),

although we are worse at detecting gradual than stepped changes (Schmerler 1976). Furthermore, our acceleration sensitivity is lower than our speed sensitivity (Gottsdanker 1956; Werkhoven et al. 1992). Acceleration information affects the latency of pursuit eye movements (Krauzlis and Lisberger 1994), but the site of acceleration computation is not clear. Neurons in macaque and pigeon pretectum encode the acceleration and speed of retinal motion (Cao et al. 2004; Das et al. 2001). Similarly, in the dorsolateral pontine nucleus (DLPN) and nucleus reticularis tegmenti pontis (NRTP) of macaque, which link cortical motion processing areas to cerebellar regions controlling smooth pursuit, many neurons are sensitive to eye acceleration and, perhaps, acceleration of retinal motion (Ono et al. 2005; Suzuki et al. 2003). Importantly, these brain stem regions are involved in oculomotor control and are unlikely to contribute directly to the perception of motion.

A candidate for the study of acceleration sensitivity is the cortical middle temporal area (MT). This specialized motion-processing region underlies perception and contains neurons tuned for speed and direction (Britten et al. 1992; Maunsell and Van Essen 1983; Nichols and Newsome 2002). Further, it projects to the acceleration-responsive pretectum and DLPN (Ibbotson and Dreher 2005). In individual MT neurons in anesthetized macaques, image acceleration is not represented in a speed-invariant manner, but it may be represented by population activity (Lisberger and Movshon 1999).

We extended the work of Lisberger and Movshon, studying the acceleration sensitivity of MT neurons in awake macaques. We used speed steps and ramps constituting constant acceleration or deceleration. The speed ramps had variable duration but matched initial and final speeds, allowing the same speed range to be tested regardless of the acceleration rate. Despite finding no strong evidence for acceleration tuning in individual cells across the population, responses to speed ramps could not be simply predicted from the speed tuning of the cells. Moreover, spiking rates evoked by acceleration are higher than those of the corresponding deceleration and preferred speeds inferred from the time at which spiking rates peak are higher for decelerations than accelerations. We show that these results can be explained by the adaptation properties of the neurons and do not reflect differential coding of acceleration and deceleration. A model incorporating adaptation and a cell's transient and sustained speed tuning that accounts for most of the individual cell responses is presented. A second, biologically plausible model provides a mechanism by which speed

Address for reprint requests and other correspondence: M. R. Ibbotson, Visual Sciences, Building 46, Research School of Biological Sciences, Australian National University, Canberra, ACT, 2601, Australia (E-mail: ibbotson@rsbs.anu.edu.au).

The costs of publication of this article were defrayed in part by the payment of page charges. The article must therefore be hereby marked "advertisement" in accordance with 18 U.S.C. Section 1734 solely to indicate this fact.

and acceleration can be extracted from the population of measured MT neuron responses.

METHODS

Surgical procedures

Behavioral and single-unit data were collected from four normal juvenile rhesus monkeys (*Macaca mulatta*), weighing 3–6 kg. All surgical and experimental procedures were performed in strict compliance with National Institutes of Health guidelines and the protocols were reviewed and approved by the Institutional Animal Care and Use Committee at Emory University. Sterile surgical procedures were carried out under aseptic conditions using isoflurane anesthesia (1.25–2.0%) to stereotaxically implant a stainless steel head stabilization post (Crist Instruments, Hagerstown, MD) and a recording chamber centered above the superior temporal sulcus (lateral 15 mm; posterior 5 mm). A scleral search coil for measuring eye movements was implanted underneath the conjunctiva of one or both eyes.

Our recording locations in MT were verified using standard histological methods. At the end of our single-unit recording studies, monkeys were sedated with ketamine-hydrochloride and deeply anesthetized with pentobarbital (80–100 mg/kg) before transcardial perfusion with physiological saline and 4% buffered paraformaldehyde. Frozen sections of the brain were cut at 50 μm , mounted on slides, and stained for Nissl substance or myelin. Our recording tracks vertically penetrated the anterior bank of the superior temporal sulcus and entered area MT after crossing the lumen of the sulcus (Fig. 1). By relating the depth of neurons, as indicated on the microdrive with histological features associated with representative electrode tracks, all neurons were assigned to area MT.

Behavioral paradigms and visual stimulation

During all experiments, monkeys were comfortably seated with the head stabilized in the horizontal stereotaxic plane. Monkeys were rewarded with fruit juice every 0.5–1 s for maintaining fixation on a red spot presented in the center of the screen. Visual stimuli were

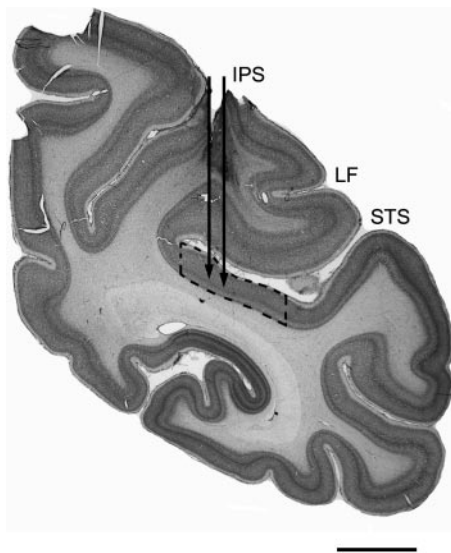


FIG. 1. Histological reconstruction of representative recording sites in MT. Nissl-stained section cut in the coronal stereotaxic plane showing the path of our electrodes entering cortex near IPS, traveling through middle superior temporal dorsal (MSTd) before reaching middle temporal (MT) cortex (dotted border). Most of our recordings were obtained within 2 mm of this level. Damaged region immediately below the IPS was caused by the guide tubes used to penetrate the dura. Abbreviations: IPS, intraparietal sulcus; LF, lateral fissure; STS, superior temporal sulcus. Scale bar = 5 mm.

rear-projected onto a tangent screen placed 61 cm from the eyes using a Mirage 2000 Digital Light Projector (Christie Digital, Cypress, CA) with resolution $1,024 \times 1,024$ pixels, frame rate 96 Hz, and mean luminance 170 cd/m^2 . Stimuli were random texture (Julesz) patterns formed of black and white squares of side length 0.8° (0.85 cm on screen) and 100% contrast. The texture pattern covered the entire $77 \times 77^\circ$ area of the tangent screen. We used large-field texture patterns to simulate the natural visual environment, which contains many spatial frequencies. Whereas the large stimuli will induce surround-suppression in many of the neurons (Born and Bradley 2005), this would be a natural consequence of locomotion through the environment and it is important to understand how neurons respond to naturalistic wide-field stimuli.

During recording, cells were assigned to area MT based on their preference for moving stimuli, their high direction selectivity, and their sensitivity to motion only in the contralateral hemifield. Before arrival in MT, electrode tracks typically passed through another area containing direction-selective neurons, shown by histological reconstructions to be area MST (middle superior temporal). On many tracks there was a distinct gap of $\leq 200 \mu\text{m}$ between MST and MT, in which it was not possible to isolate cells.

We studied the physiological responses of 91 units in four monkeys. Of these, 45 were clearly recordings from single neurons based on their regular and stable spike shape and size and their large signal-to-noise ratios. The remaining units were most likely single cells based on spike shape, but were more variable in spike amplitude. For the purposes of this analysis, no significant differences were observed between the responses of cells with stable or more variable spike amplitudes. We initially determined each cell's preferred direction by presenting 0.5-s periods of motion in eight to 16 uniformly separated directions while the monkey fixated a central spot. The preferred direction was determined from the direction giving the largest spiking response averaged over the period of motion. Subsequently, all stimuli moved in the cell's preferred direction while the animal fixated. Three types of motion stimuli were presented. First, we tested speed tuning using six to eight constant speeds in the range 4–240°/s. Motion periods lasted 0.5–3 s and were preceded and followed by presentation of the same, stationary texture for ≥ 0.5 s. Second, we tested acceleration sensitivity using speed ramps of variable duration but a fixed peak speed of 240°/s. These tests had symmetric speed profiles: stationary for 1 s; acceleration to 240°/s; constant speed for 1 s at 240°/s; deceleration to 0°/s at the same rate as the acceleration period; stationary for 1 s. Accelerations and decelerations of 60, 80, 120, 240, 480, 960, and 2,400°/s² taking from 0.1 to 4 s to reach the 240°/s plateau were tested. Finally, we used speed ramps with acceleration and deceleration periods of fixed 1-s duration. As with the tests with a fixed peak speed, symmetric speed profiles were used. Accelerations and decelerations of 10, 20, 40, 80, 160, and 240°/s² were used. For all stimuli, eight to 32 repetitions were performed; however, because of time constraints or unstable isolations, not all tests were carried out on all cells.

Eye position and action potential collection and analysis

Unit activity was sampled at 25 kHz using iron-tipped, epoxy-coated tungsten electrodes with impedance 1–4 M Ω before iron coating (FHC, Brunswick, ME). Single-unit action potentials were detected on-line with a hardware window discriminator or software template matching algorithm (Alpha-Omega, Nazareth, Israel). In addition, we checked action potential shape and detection off-line using the Wavemark template matching provided in Spike2 (CED, Cambridge, UK). For off-line analysis, neuronal responses were represented as spike density functions (SDFs) with 1-kHz resolution (Price et al. 2005). These were generated by convolving a delta function at each spike arrival time with a Gaussian window ($\sigma = 3$ ms) and then averaging responses to individual stimulus presentations, including only portions of the response during which the eye position

was within 3° of the desired fixation point. In addition, we ignored responses 100 ms after the eye position reentered the desired 3° fixation window. Eye position was monitored in two dimensions using a magnetic coil system (CNC Electronics, Seattle, WA) and sampled at 1 kHz with 16-bit precision using a Power 1401 (CED). The relatively large 3° fixation window allowed the inclusion of the majority of the response to each stimulus trial. Even though the acceptance window is quite large, across the four monkeys, eye position was within 0.5 and 1° of the fixation point 90 and 96% of the time, respectively. Further, because of the wide-field stimulus, eye movements did not move the stimulus outside the cell's receptive field.

A synchronization pulse presented in the blanking interval before the start of the first frame of each stimulus was used to align stimulus presentation and the recording of eye position and action potentials. Response latencies for stimulus-evoked responses were calculated relative to this synchronization pulse. We calculated a response threshold based on the mean + 3 SDs of the neuron's spontaneous firing rate. The spontaneous rate was averaged from ≥ 48 periods of 500-ms duration while the monkey fixated the stationary texture stimulus, before testing the responses to passive motion. Response latencies were then taken as the first time when the spiking rate in the SDF exceeded this threshold and remained above the threshold for the subsequent 25 ms. This represents a more rigorous implementation of a protocol used previously to measure latencies in area MT (Raiguel et al. 1999). Relative delays in the stimulus trigger, window discriminator, and software template matching system used to identify action potentials were always < 1.6 ms, and thus they do not significantly affect the latency calculations. Because latencies were measured from SDFs calculated after convolution of spike arrival times with a Gaussian window ($\sigma = 3$ ms), the measured latencies are 2–4 ms lower than the actual latencies. Importantly, however, these latency reductions are consistent across all cells.

The responses to speed steps were calculated in two ways. First, the sustained response was found by averaging the firing rate from 200 ms after motion onset to the end of motion. Second, the spiking rate was averaged in all 24-ms windows in the first 200 ms after motion onset, using 1-ms steps in the window start time. The largest average spiking rate recorded in any of these 200 windows was taken as the cell's transient response. The variable start time of the averaging window used to calculate transient responses allows for speed-dependent and cell-dependent variations in latency. Responses to speed ramps were calculated in similar ways. First, the sustained response was found by averaging the firing rate in a latency-adjusted window of the same duration as the speed ramp. Latency adjusting refers to the fact that we delayed the start of the averaging window by the cell's latency at its preferred speed, to account for the period of time before the cell begins to respond. Second, as when finding the transient speed tuning, we used a sliding window of 24-ms length with 1-ms resolution to find the highest average spiking rate in any 24-ms window throughout the ramp period. The time of the maximum response was taken as the center of the window in which the highest averaged spiking rate was recorded.

For each cell, the responses to constant speeds and accelerations were fit with a skewed-Gaussian function after subtracting the spontaneous firing rate

$$R_x = A \exp \left\{ - \left[\frac{\log(x/x_{\text{pref}})}{B + C \log(x/x_{\text{pref}})} \right]^2 \right\}$$

where R_x is the response at speed or acceleration x ; A controls the amplitude; x_{pref} is the cell's preferred speed or acceleration, at which the peak spiking rate A occurs; B is the bandwidth; and C controls the skew of the curve.

RESULTS

Responses to speed steps and speed ramps

A neuron's speed tuning is typically characterized by finding the response of neurons to motion in the preferred direction when speed is stepped from 0°/s to the desired speed, then held constant for a given period. Figure 2 shows SDFs for two cells tested with steps in a single monitor frame (10 ms) from zero speed to values of 10–240°/s. The transient (peak 24 ms) and sustained (200 ms after motion onset to end of motion) speed-tuning curves are shown below the SDFs for each cell. Methods for probing acceleration tuning are not well established, and thus we chose to test for acceleration tuning in conceptually the same manner as the testing of speed tuning. Using accelerating and decelerating speed ramps from 0 to 240°/s and 240 to 0°/s lasting 0.1 to 4 s we tested seven acceleration rates from 60 to 2,400°/s². The SDF responses to these stimuli for the same cells shown in Fig. 2 are presented (Fig. 3). Conceptually similar methods to the transient and sustained speed tuning were applied to the acceleration responses. The insets in Fig. 3 show the maximum (peak 24 ms) and sustained (averaged over the latency-adjusted period of acceleration) responses measured for the range of accelerations and decelerations.

Speed tuning was clearly present in all cells tested using a range of criteria. By *speed tuning* we mean that responses increase to a peak as speed increases, then decrease as speed

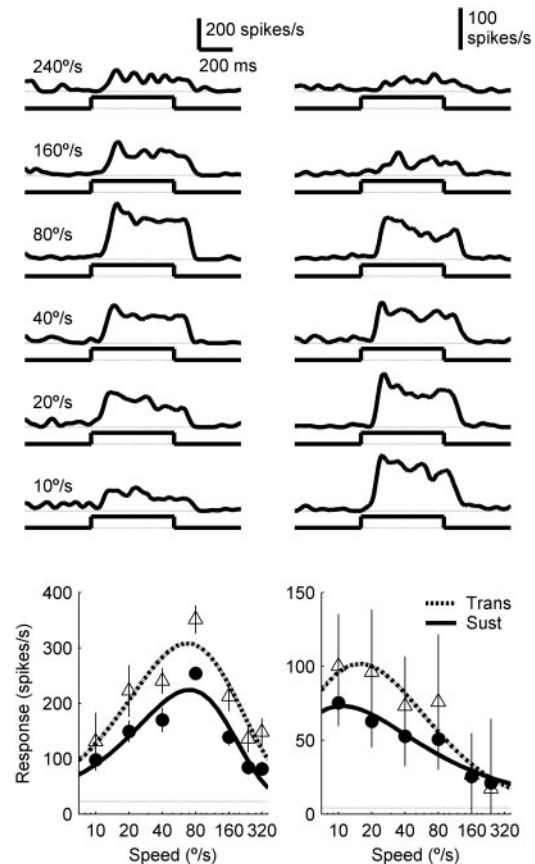


FIG. 2. Responses to speed steps for 2 cells. *Top plots*: responses to steps in stimulus speed of 10–240°/s lasting 0.5s. *Bottom plots*: measured transient (Δ , peak 24 ms) and sustained (\bullet , 200–500 ms) speed-tuning curves and skewed-Gaussian fits to these data points.

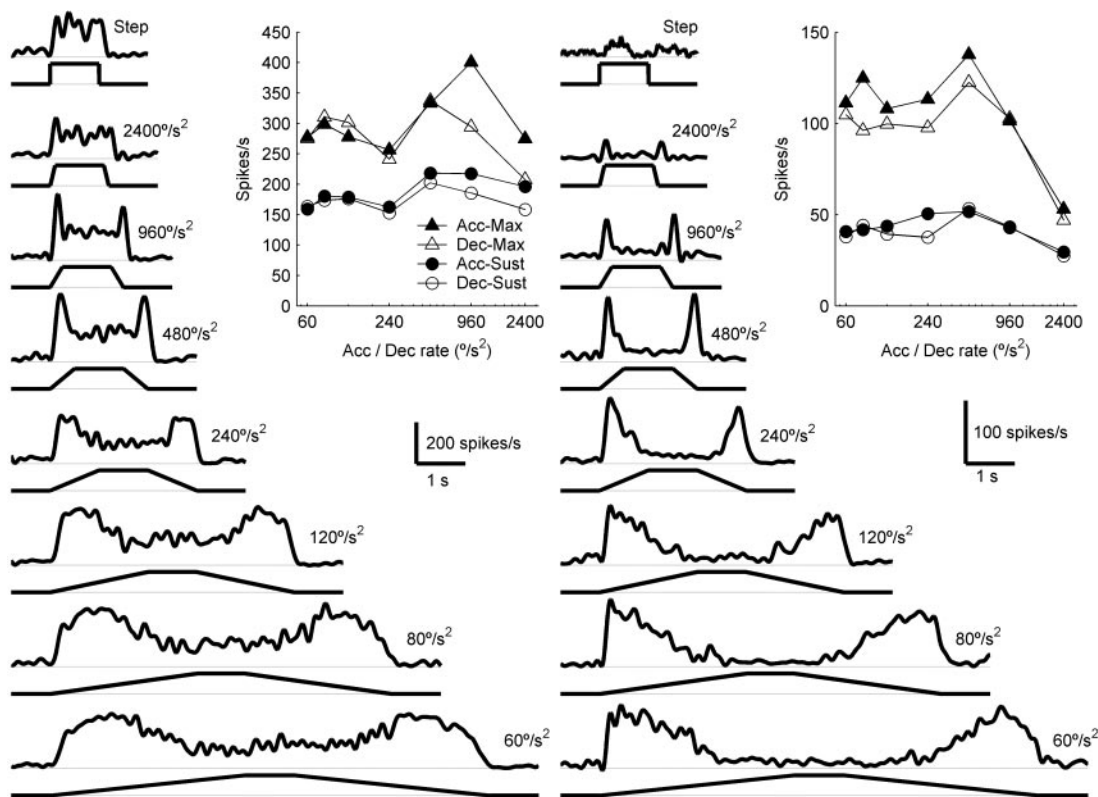


FIG. 3. Responses to speed ramps for the same 2 cells shown in Fig. 2. Main plots show spike density functions (SDFs) for responses to ramps in stimulus speed of 60–2,400°/s² to a plateau speed of 240°/s. Topmost SDFs are associated with a step in stimulus speed from 0 to 240°/s. Insets: measured maximum (▲, Acc; △, Dec) and sustained (●, Acc; ○, Dec) tuning curves for the responses to periods of acceleration and deceleration.

increases beyond that level, thus forming an inverted U-shaped response tuning function. First, across the population, cells had a range of preferred speeds covering the full range of speeds tested from 4 to 240°/s. Second, all cells showed significant variation in either their transient or sustained speed tuning across the range of speeds tested (one-way ANOVA, $P < 0.01$). Third, median R^2 values for fits of a skewed Gaussian to the speed-tuning functions derived from transient and sustained responses were 0.93 and 0.94, respectively, indicating that across the population, speed-tuning curves are satisfactorily described by an inverted-U shape.

In contrast, acceleration tuning does not appear to be a fundamental property of cells in area MT. Only 50% of cells show significant variation in their maximum or sustained responses across the range of accelerating and decelerating speed ramps tested (60–960°/s²; one-way ANOVA, $P < 0.05$). Responses to 2,400°/s² were omitted from this analysis because the responses were highly variable as a result of the short stimulus duration. The median R^2 value for fits of a skewed Gaussian to the acceleration and deceleration responses was 0.64. This low value reflects the fact that for many cells, responses could not be fit satisfactorily by an inverted-U shape. Thus we checked simply for *systematic* variations across the range of accelerations tested.

Responses were defined as varying systematically if they showed a monotonic increase, then monotonic decrease in magnitude as acceleration increased, or if they showed a purely monotonic change in magnitude as acceleration increased. Cells that showed oscillatory changes in response size with increasing acceleration did not show systematic variation (e.g.,

Fig. 3). For those cells showing *significant* variation in their responses across a range of accelerations, only 62 and 45% showed *systematic* variation in their maximum and sustained responses, respectively, across the full range of accelerations. In contrast, 79% of cells showed systematic variation in both their transient and sustained responses to stepped changes in speed.

Speed tuning: timing is critical

The time windows used to measure speed tuning critically affect the size and shape of the speed-tuning curve, which results from the speed dependency of latency and the adaptation evident in the responses to even quite short stimuli (e.g., Fig. 2). For individual cells and across the population, latencies typically decreased with increasing speed (Fig. 4, A and B); however, these variations predominantly occur for speeds $< 20^\circ/\text{s}$. Preferred speeds and amplitudes were obtained from the parameters of a skewed-Gaussian fit to the transient and sustained speed-tuning curves. After subtracting spontaneous firing rates, the median ratio of transient:sustained responses was 2.04 (25th and 75th percentiles: 1.60, 2.80), demonstrating the large response decline resulting from adaptation (Fig. 4C). Transient responses indicated lower preferred speeds than sustained responses in 70% of cells (49/70, Fig. 4D). However, the two measures show reasonable linear correlation on a log-log plot ($R^2 = 0.68$), with the linear regression line having a slope of 1.0.

Are acceleration and deceleration coded differently?

Although 50% of cells show little difference between the responses to accelerations of different rates, there are quanti-

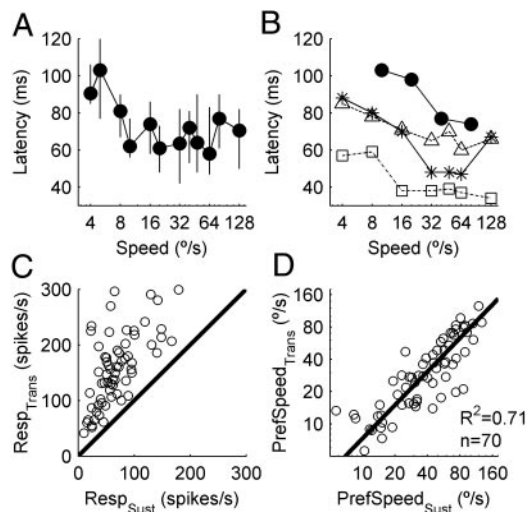


FIG. 4. Speed-tuning properties from the population ($n = 70$ cells). Speed dependency of latencies is shown for the population of cells (A) and for 4 individual cells (B). Markers in A show median latencies, with error bars indicating 25th and 75th percentiles. C: comparison of response amplitude at the preferred speed associated with transient and sustained measures of speed tuning. In each case, spontaneous firing rate has been subtracted. Solid line shows the line of unity. D: comparison of the preferred speeds associated with sustained and transient speed tuning. Solid line shows linear regression $y = 1.03x - 0.42$.

tative differences between the responses to accelerations and decelerations of the same rate. Figure 5 compares the sustained (A) and maximum (B) responses to accelerations and decelerations of the same rate in 329 tests performed on 78 cells. Sustained responses show very strong correlation ($R^2 = 0.84$) and linear regression minimizing perpendicular distances produces a line with a slope of 0.91 and an offset of only 1 spike/s. This indicates that sustained responses are slightly higher for acceleration than deceleration, although there is no significant difference across the population of cells (Fig. 5A). Maximum responses are also strongly correlated ($R^2 = 0.78$), with the regression line having a slope of 0.85, indicating that larger peak firing rates are produced by acceleration than by deceleration (Fig. 5B).

We defined an acceleration–deceleration tuning index (ADTI) that compared the maximum and sustained responses to speed ramps

$$\text{ADTI} = (R_{\text{Acc}} - R_{\text{Dec}}) / (R_{\text{Acc}} + R_{\text{Dec}})$$

An ADTI close to 0 indicates that there is no difference between the response to acceleration and deceleration. ADTIs >0 indicate a preference for acceleration, whereas ADTIs <0 indicate larger responses to deceleration. The distributions of ADTIs were unimodal across the population, with median ADTIs of 0.12 and 0.07 for the distributions of maximum and sustained responses, respectively (Fig. 5, C and D). Despite the rightward skew in values of ADTI, only the maximum responses were significantly >0 ($P < 0.01$, Student's t -test), demonstrating a preference for acceleration across the population when using this measure.

To characterize the population's preference for acceleration or deceleration at different rates, we averaged the responses to each acceleration and deceleration rate across the population of cells (Fig. 5, E and F). Responses were first normalized relative to the largest of the peak responses to acceleration and decel-

eration. Asterisks under each pair of data points indicate where they are significantly different. Significant differences are evident only in the maximum responses. The three measures comparing responses to acceleration and deceleration discussed above demonstrate that, although the sustained responses to a period of the same rate of acceleration and deceleration are closely matched, the maximum response profile to acceleration and deceleration.

Predicting preferred speed from speed ramps

Up to this point we have assessed differences in firing rate associated only with acceleration and deceleration tests. Here we compare the preferred speed measured from steps in stimulus speed with that inferred from the responses to acceleration and deceleration. Preferred speeds associated with the responses to speed ramps were estimated by finding the time when firing rate peaked, adjusting for the cell's latency, and finding the corresponding stimulus speed. This preferred speed was calculated for each of the seven acceleration and deceleration rates tested for every cell. Thus for each cell, we could have ≤ 14 estimates of the preferred speed. Figure 6 compares

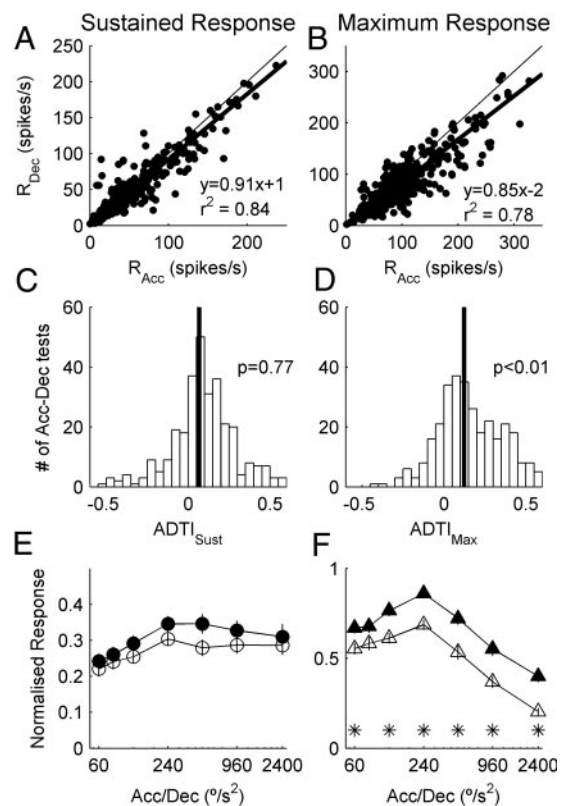


FIG. 5. Sustained (left column) and maximum (right column) responses to accelerations and decelerations of 60 – $2,400^\circ/\text{s}^2$. A and B: comparison of sustained and maximum responses for every acceleration rate tested with every cell ($n = 329$ tests). Thin and thick lines show the lines of unity and result of linear regression, respectively. C and D: distribution of acceleration–deceleration tuning index (ADTI), calculated for every test shown in A and B. Vertical black lines indicate the median value. P values show the significance of a t -test used to determine whether the population is significantly shifted from 0. E and F: population average of the sustained and maximum responses to each acceleration (\blacktriangle , \bullet) and deceleration (\triangle , \circ) rate. Asterisks below a pair of data points indicate that they are significantly different ($P < 0.05$).

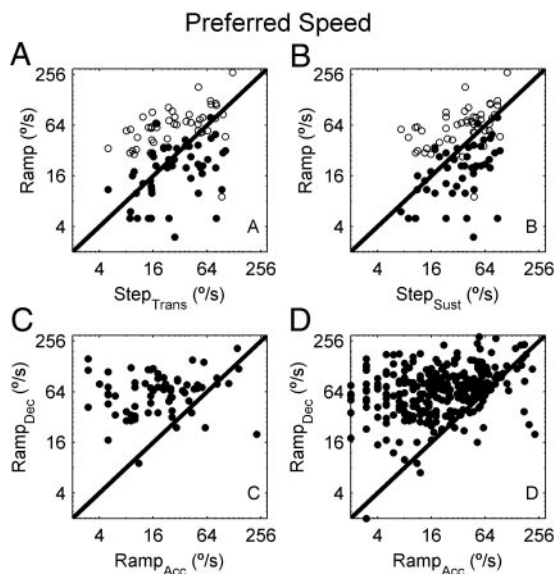


FIG. 6. Preferred speeds measured from speed steps and inferred from speed ramps (acceleration and deceleration). Comparison of preferred speed inferred from speed ramps of $240^\circ/\text{s}^2$ with transient (A) and sustained (B) responses to speed steps. Preferred speeds associated with acceleration (\bullet) and deceleration (\circ) are shown. Comparison of preferred speeds inferred from accelerating and decelerating ramps of $240^\circ/\text{s}^2$ (C) and for all rates tested (D).

the estimated preferred speed measured from the response to acceleration (\bullet) and deceleration (\circ) at $240^\circ/\text{s}^2$ with the preferred speed indicated by transient (A) and sustained (B) responses to speed steps. In general there is poor correlation between the preferred speeds inferred from speed ramps and speed steps, but one characteristic is striking: the preferred speed indicated by deceleration is higher than that indicated by the transient and sustained speed tuning in 89 and 78% of cells, respectively. This is indicated by the open circles (deceleration) being higher on the y-axis than the filled circles (acceleration) in Fig. 6, A and B. This trend was evident for preferred speeds inferred from all acceleration and deceleration rates.

Figure 6C compares the preferred speeds inferred from the response to $240^\circ/\text{s}^2$ acceleration and deceleration for 77 cells. In 89% of cells, the preferred speed indicated by deceleration is higher than that indicated by acceleration and across the population these differences are significant ($P < 0.01$, Student's *t*-test). Figure 6D shows the same comparison of preferred speeds, but for all acceleration rates tested (333 tests on 77 cells), indicating that the difference in preferred speeds is significant regardless of the acceleration rate. The difference in preferred speed is associated with the peak firing rate evoked by the deceleration test occurring earlier than would be expected from the response to acceleration. From Fig. 6C, the mean difference in preferred speeds indicated by acceleration and deceleration ramps of $240^\circ/\text{s}^2$ is $36^\circ/\text{s}$, corresponding to a difference in the time of peak spiking rate of 0.15 s ($0.15 = 36/240$).

Effect of eye movements on responses to motion

As a control, we assessed the influence of eye movements on the responses to speed steps and ramps. Figure 7 shows horizontal eye traces associated with three rightward moving stimuli: (A) a $40^\circ/\text{s}$ step; (B) an $80^\circ/\text{s}^2$ ramp; and (C) a $240^\circ/\text{s}^2$

ramp. Eye movements were characterized by fixation with stable eye position interrupted by low-speed tracking eye movements in the direction of stimulus motion (positive deflections on the traces shown) and counter-directed saccades (negative deflections). These eye movements are consistent with very low gain optokinetic nystagmus (OKN) that is largely suppressed by fixation (e.g., Pola et al. 1995). Eye tracking speeds were typically $<2^\circ/\text{s}$, and thus they are unlikely to influence the neural responses to motion because of their very low gain.

It has been shown that MT neurons are sensitive to the speed and direction of saccades (Bair and O'Keefe 1998; Price et al. 2005). The probability of saccades occurring within 50-ms bins relative to stimulus onset is shown in histograms below each set of eye traces. Peaks in the histograms show that saccades were most likely to occur 250–350 ms after motion onset, regardless of the stimulus speed or acceleration rate. The

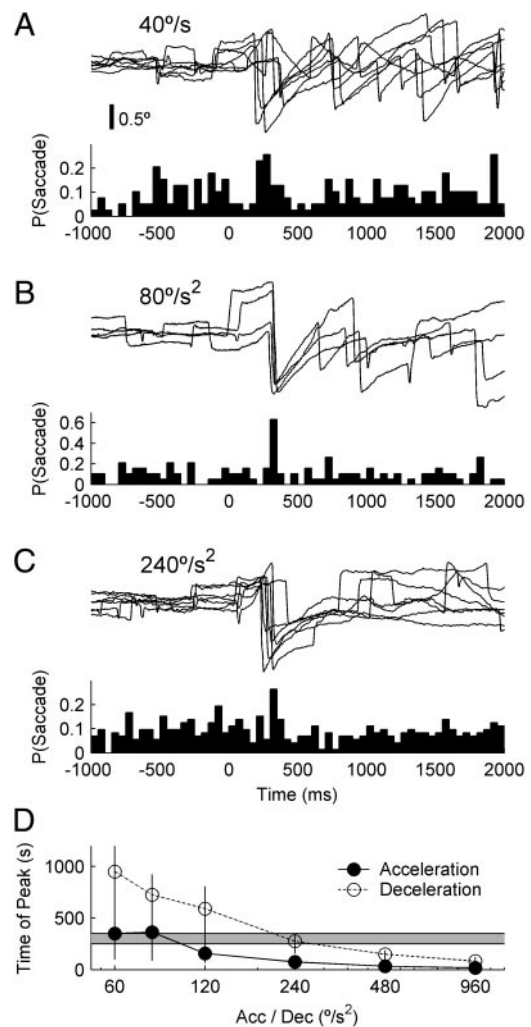


FIG. 7. Horizontal eye positions and the probability of saccade occurrence for a $40^\circ/\text{s}$ speed step (A), $80^\circ/\text{s}^2$ speed ramp (B), and $240^\circ/\text{s}^2$ speed ramp (C). In each case motion started at time 0 ms. Stimulus motion and tracking eye movements are represented by upward deflection on the traces. Time at which response rate peaked relative to the time when the ramp speed was $0^\circ/\text{s}$ is shown for accelerating and decelerating speed ramps (D). Horizontal shaded region indicates the period 250–350 ms after motion onset, when saccades were most likely to occur. Saccade probability histograms were collated from 39 (A), 19 (B), and 72 (C) eye traces.

saccades in this time window most likely represent the first time-locked, counter-directed saccade in the OKN cycle. After saccades in this time window, eye movements occur more randomly throughout the stimulus motion period. The short duration and displacement of saccades suggests that their effects on neural responses will be negligible. Apart from the first saccade after motion onset, eye movements were randomly directed and their effects should average out across multiple stimulus repetitions. Importantly, saccades occurred only in the period 250–350 ms after motion onset in 25–65% of trials. To determine whether the alignment of saccades across stimulus repetitions had a significant effect on the responses to motion, we calculated the median time at which the firing rate peaked, for all acceleration rates (Fig. 7D). Times are expressed relative to when the stimulus speed is 0°/s: the time of motion onset for acceleration and time of motion end for deceleration. Both acceleration and deceleration measures show a clear trend of shorter times to peak response with increasing ramp rate. The horizontal shaded bar indicates the window in which saccades were most frequently observed in the responses to acceleration. This time range was independent of ramp rate and typically later than the times when responses to acceleration peaked. This clearly demonstrates that saccades are unlikely to influence the time at which responses to acceleration reach a maximum.

How does motion history affect speed tuning?

The previous section attempted to predict a cell's preferred speed using the response to speed ramps. To investigate the effects of acceleration and motion history on the responses to stable speeds, we recorded the responses of cells to speed plateaus lasting 1 s reached after 1 s of acceleration. In each case, the plateau speed was the final value of the speed ramp (i.e., a 1-s speed ramp at A°/s^2 reaches a final speed of A°/s , which is then presented for 1 s). We compared the sustained responses to the speed plateaus, measured in the time window 0.1–1 s after reaching the plateau speed, with transient and sustained responses to the speed steps that we have used previously. Figure 8, *A* and *B* shows the speed-tuning curves of two cells generated using the transient and sustained responses to speed steps, and the sustained response to speed plateaus after acceleration. Although there is close agreement in the shape of the speed-tuning curves, the absolute spiking rates associated with the sustained responses to the speed plateau after acceleration are lower than the responses to speed steps. We tested 34 cells with both speed steps and speed ramps, although only 21 cells had isolations that were deemed stable across the entire period of recording. For these 21 cells, we fitted the three speed-tuning curves with a skewed Gaussian, and found the peak amplitude and preferred speed associated with the fits.

In the majority of cells, both the magnitudes of the transient and sustained responses to speed steps were higher than the responses to the speed plateaus after acceleration (Fig. 8, *C* and *D*). The spiking rate response to the speed plateau showed similar correlation with both the sustained response rate ($R^2 = 0.67$) and the transient response rate ($R^2 = 0.64$). In both cases, regression lines had slopes >1 , indicating that the responses to speed steps without prior motion exposure were greater than those evoked by the speed plateaus after acceleration. Preferred

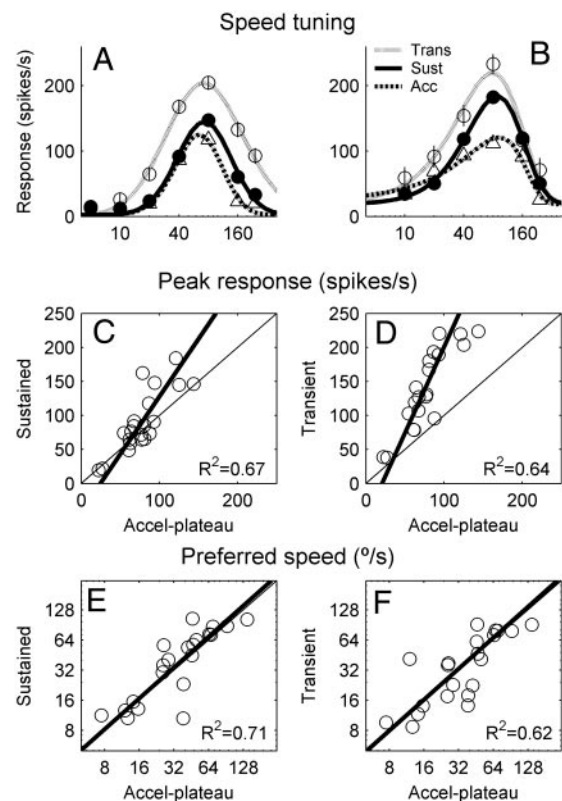


FIG. 8. Speed tuning associated with speed steps and speed plateaus after 1 s of acceleration. *A* and *B*: speed-tuning curves for 2 cells measured using transient and sustained responses to speed steps and sustained responses to speed plateaus after acceleration. Peak response amplitudes (*C*, *D*) and preferred speeds (*E*, *F*) are compared for responses to speed steps and speed plateaus after acceleration.

speeds associated with the speed plateaus were also reasonably correlated with preferred speeds associated with sustained ($R^2 = 0.71$) and transient responses ($R^2 = 0.62$) to speed steps (Fig. 8, *E* and *F*). The slopes of the regression lines were 1.11 (sustained) and 1.09 (transient), highlighting the similarity in preferred speeds. This suggests that the period of acceleration before the test phase in which speed tuning is measured does not significantly affect the measurement of the preferred speed, but significantly reduces the spiking rate elicited by the subsequent stimuli.

In previously described tests, acceleration was always preceded by a period of zero motion but decelerations were preceded by periods of acceleration and constant speed. Therefore motion adaptation cannot affect the early responses to acceleration, but may affect the responses to deceleration. To determine whether motion history and adaptation affect the responses to acceleration, we used stimuli with two periods of acceleration at $160^\circ/s^2$ separated by 3-s adapting periods (Fig. 9A). The speed in the adapting period was 0 or $40^\circ/s$, chosen because it is close to the preferred speed for all the cells tested. An example of the responses from one neuron to the two stimuli is shown in Fig. 9B. The response evoked by the second period of acceleration is similar to that evoked by the first period only if the adapting speed is $0^\circ/s$. After adaptation at $40^\circ/s$, the acceleration response is considerably attenuated. These findings were consistent across a population of 19 cells tested. Maximum responses evoked by the first and second

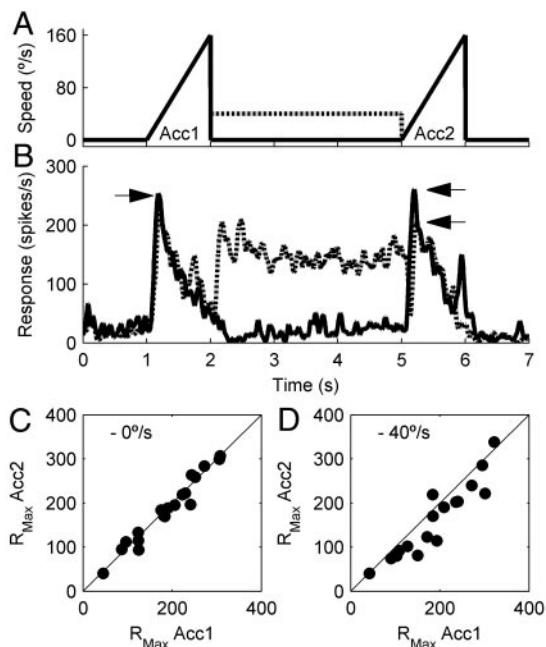


FIG. 9. Responses to two $160^\circ/\text{s}^2$ acceleration periods (Acc1, Acc2) separated by a 3-s adaptation period at 0 or $40^\circ/\text{s}$. Stimulus speed profiles (A) and the corresponding SDFs (B) are shown for one cell. Arrows in B indicate the amplitudes of the maximum responses evoked by the two stimuli. For the response to Acc1, the maximum responses are the same for the 2 stimulus conditions. For responses to Acc2, the bottom arrow indicates the maximum response after the $40^\circ/\text{s}$ adaptation period. Maximum responses of 19 cells evoked by the 2 acceleration periods are compared for adapting speeds of $0^\circ/\text{s}$ (C) and $40^\circ/\text{s}$ (D).

acceleration periods are not significantly different when the adapting speed is $0^\circ/\text{s}$ ($P = 0.19$, Student's t -test, Fig. 9C). However, when the adapting period presents motion at $40^\circ/\text{s}$, responses to the second acceleration period are significantly

reduced ($P < 0.001$, Fig. 9D). The average reduction in amplitude of the maximum response was $85 \pm 15\%$ (SD), demonstrating the effect of adaptation on responses to acceleration.

Transient and sustained speed tuning provide poor fits to acceleration responses

The results thus far have indicated that acceleration tuning is not a characteristic property of cells in area MT. Despite this, the responses to acceleration and deceleration are clearly different, suggesting that prior motion history affects the responses of neurons. A linear model of a system that is exclusively speed sensitive and that does not code acceleration would predict that the transient and sustained speed-tuning curves represent upper and lower limits on the response to a speed ramp. The actual response would be expected to fall between these limits, depending on the adaptation state of the cell. Figure 10 shows the responses of four cells to acceleration and deceleration ramps of $240^\circ/\text{s}^2$. The upper and lower boundaries of the shaded gray background indicate the responses predicted from the transient and sustained speed-tuning curves. These were adjusted for the cell's latency at the preferred speed and matched to the instantaneous stimulus speed. It is evident that neither the transient nor sustained speed-tuning curves provide good representation of the neuronal response to acceleration when used in isolation.

We assessed the proportion of time that a neuron's spiking rate evoked by acceleration and deceleration at $240^\circ/\text{s}^2$ fell within four response ranges associated with the cell's speed tuning: 1) the 68% confidence interval for the skewed-Gaussian fit to the transient and 2) sustained speed-tuning curves (Fig. 11, A and B); 3) below the fitted transient speed-tuning curve (Fig. 11C); and 4) above the sustained speed-tuning

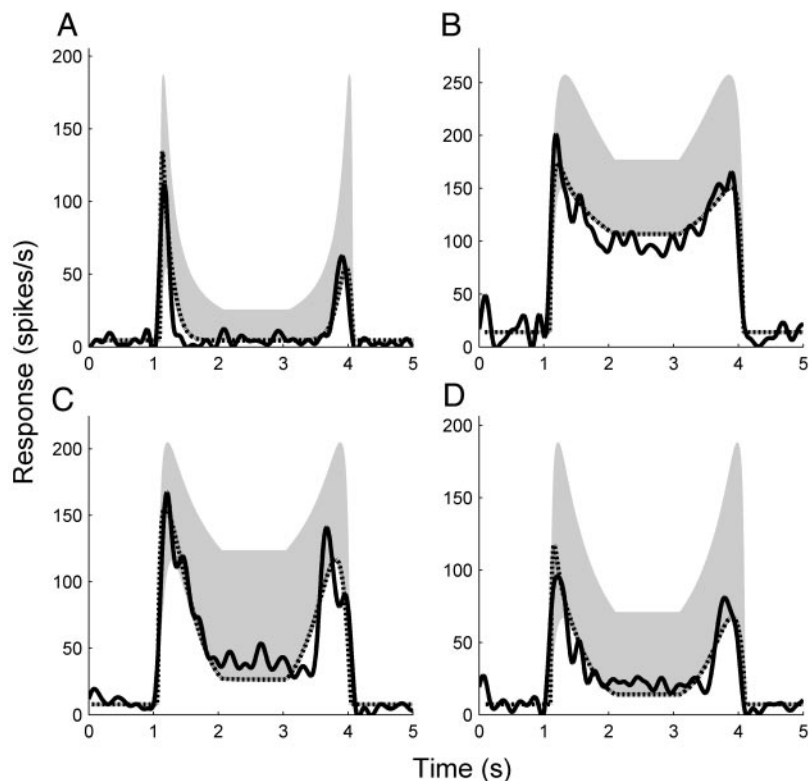


FIG. 10. Neuronal and modeled responses for 4 cells, generated by a stimulus accelerating at $240^\circ/\text{s}^2$ for 1 s, maintaining $240^\circ/\text{s}$ for 1 s then decelerating at $240^\circ/\text{s}^2$ for 1 s. Solid line: neuron response; dotted line: model prediction; boundaries of shaded background: response prediction based on transient and sustained responses to speed steps.

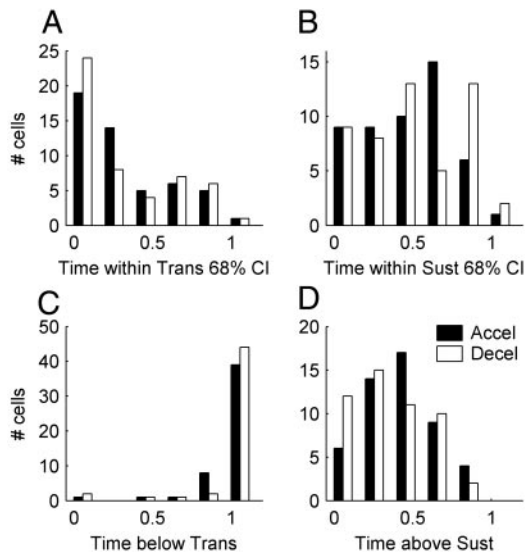


FIG. 11. Measures of the time during which responses to acceleration are within boundaries defined by transient and sustained speed-tuning curves ($n = 51$ cells). Proportion of time in which the response to acceleration lies within the predicted boundaries is based on a 68% confidence interval for the transient (A) and sustained (B) speed-tuning curves. C and D: proportion of time in which the acceleration responses lie below the transient speed-tuning curve and above the sustained speed-tuning curve, respectively.

curve (Fig. 11D). A proportion of 1 indicates that the neuron's acceleration response falls entirely within the tested response range; conversely, a proportion of 0 indicates that the acceleration response falls entirely outside the tested range. Figure 11, A and B demonstrates that very few cells have the majority of their acceleration and deceleration responses predicted entirely by the transient or sustained speed-tuning curve. However, Fig. 11C shows that for acceleration and deceleration responses 73 and 88% of cells, respectively, have >90% of responses fall below the transient speed-tuning curve. Thus the transient speed-tuning curve provides a good upper boundary for the predicted response of the cell to acceleration. However, the sustained speed-tuning curve provides a poor lower boundary for predicting acceleration responses, with only one cell having >90% of its acceleration response above the sustained speed-tuning curve (Fig. 11D). This finding combined with the findings from the previous section, assessing preferred speeds and firing rates measured in response to speed steps and speed plateaus after acceleration, indicate that adaptation strongly affects a neuron's firing rate.

Modeling speed tuning with adaptation

Although transient and sustained speed-tuning curves on their own represent poor predictors of the responses to acceleration, the transient speed-tuning curve represents a good upper boundary for any predicted response. In addition, our results have suggested that: 1) periods of acceleration evoke larger maximum responses, but similar sustained responses compared with deceleration periods of the same rate; 2) cell responses show little significant or systematic variation across a range of acceleration or deceleration rates; and 3) the preferred speed inferred from the responses to deceleration was higher than that predicted from acceleration responses or steps in stimulus speed.

We developed a simple adapting model of speed tuning in a cell to relate these characteristics to the transient nature of individual cell's responses to speed steps. The model incorporates only a cell's transient and sustained speed-tuning curves and an adaptation rate (τ) governing how quickly the cell's transient response declines to the sustained response. The model cell's adaptation state (AS) is a value between 0 and 1, calculated at each instant in time by

$$AS_{t+\delta t} = AS_t \exp(-\delta t/\tau) \quad \text{if } R_t > R_{\text{thresh}}$$

$$AS_{t+\delta t} = 1 + (AS_t - 1) \exp(-\delta t/\tau) \quad \text{if } R_t < R_{\text{thresh}}$$

where $AS_{t+\delta t}$ and AS_t are the adaptation states at time $t + \delta t$ and t , respectively; τ is the adaptation rate of the cell; R_t is the firing rate response at time t ; R_{thresh} was set to 5 spikes/s and is a threshold firing rate governing whether the cell is adapting ($AS_{t+\delta t} < AS_t$) or recovering ($AS_{t+\delta t} > AS_t$).

The cell's firing rate at each point in time is then given by

$$R(t + t_{\text{late}}) = AS_t \times R_{\text{trans}}(s_t) + (1 - AS_t) \times R_{\text{sust}}(s_t)$$

where s_t is the stimulus speed at time t , t_{late} is the cell's latency at the preferred speed, and $R_{\text{trans}}(s_t)$ and $R_{\text{sust}}(s_t)$ are the transient and sustained responses to speed s_t .

The basic rationale of the model is that the adaptation state is firing-rate dependent. Thus if the cell's firing rate is high, the cell adapts more, making the responses tend toward the sustained speed-tuning curve. If the cell's firing rate is low, the cell recovers, making the responses tend toward the transient speed-tuning curve.

The value of τ governing the adaptation rate was initially inferred from the time constant of exponential fits to each cell's responses to steps in stimulus speed. This method was unsatisfactory because the adaptation rate is speed dependent and single time-constant exponential functions provided poor fits to the data. Thus we chose the value of τ that maximized the coefficient of determination (R^2) between the model prediction and the entire acceleration-plateau-deceleration stimulus period.

Sample outputs of the model (dashed lines) for four cells responding to acceleration and deceleration ramps of $240^\circ/s^2$ are shown in Fig. 10, superimposed on the raw SDFs (solid line). In all cases it is clear that the model closely captures the peak spiking rates and adaptation profiles better than the predictions based solely on the cell's speed tuning (gray background). For example, the cell shown in Fig. 10A has significantly larger maximum responses to acceleration than deceleration. By adapting from the cell's transient rate of firing to close to its sustained rate of firing for a given speed, the model is able to re-create this response profile. One aspect of the neuronal data that is not captured relates to responses that fall below the sustained speed tuning (evident in Fig. 10, C and D from 3 to 3.5 s). This is attributed to the model's firing rate being limited to fall between the bounds imposed by the cell's transient and sustained speed-tuning curves (shown in gray). We found that the decay in firing of real neurons is not perfectly exponential, as outlined in the previous paragraph, which might explain the difference between the real data and the model (e.g., the decay might be better described by the product of two exponentials). To keep the model simple, we did not incorporate more complex response decay profiles.

The quality of the model was assessed by cross-correlating the predicted model response with the neuronal spiking response. This is a form of cross-validation using the holdout method: *training data* acquired from each neuron's speed tuning are used to predict the *testing data* associated with the responses to speed ramps (e.g., Stone 1974). Periods of acceleration and deceleration were assessed separately. Coefficients of determination were calculated both for the adapting model and for the nonadapting models based entirely on either the transient or sustained speed tuning. Figure 12, *A* and *B* compares the coefficients of determination associated with the adapting and nonadapting models for acceleration. The majority of points lie above the line of unity, indicating that the adapting model outputs provide significantly better fits to the neuron responses to acceleration than either the transient or sustained speed tuning alone ($P < 0.01$, paired *t*-test).

Figure 12, *C* and *D* shows the same comparison for the neural and modeled responses to deceleration. Although the model provides qualitatively better fits than the transient speed-tuning response in 78% of cells, these differences are not significant ($P = 0.1$, paired *t*-test). Further, the model is no better than the sustained speed-tuning response at predicting the deceleration response (Fig. 12*D*). This is because the relatively short time constants ($\tau = 0.01$ – 2 s) used in the model mean that the adaptation state has reached its floor of 0 by the time the deceleration is presented. Thus the model response to deceleration closely matches the cell's sustained speed tuning. In summary, the model provides significantly better fits to the full neuronal responses, which include both acceleration and deceleration, than responses predicted from either the transient or sustained speed tuning.

The basic form of this model incorporated only a single measure of latency, associated with the latency to the cell's preferred speed. Figure 4, *A* and *B* demonstrates that latencies show strong speed dependency, with response latencies de-

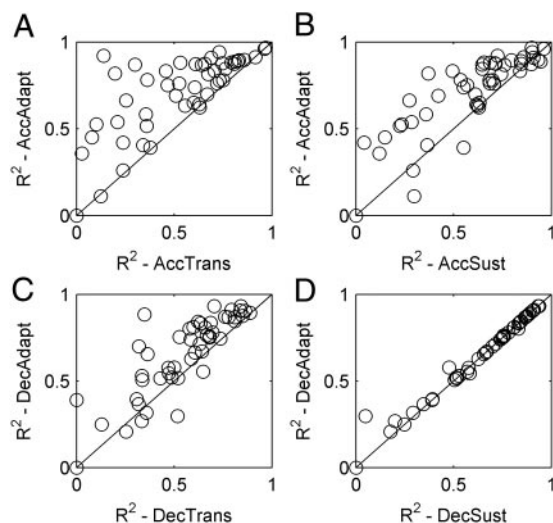


FIG. 12. Quantification of model performance. Each R^2 value represents the coefficient of determination associated with a model output and a neuron's response to a period of acceleration (*A*, *B*) or deceleration (*C*, *D*) at $240^\circ/\text{s}^2$. Model outputs were calculated using only a cell's transient speed-tuning information (*x*-axis in *A* and *C*), only a cell's sustained speed-tuning information (*x*-axis in *B* and *D*), or a cell's transient and sustained speed-tuning information and incorporating adaptation (*y*-axis in each plot). Higher R^2 values indicate a better model fit to the data.

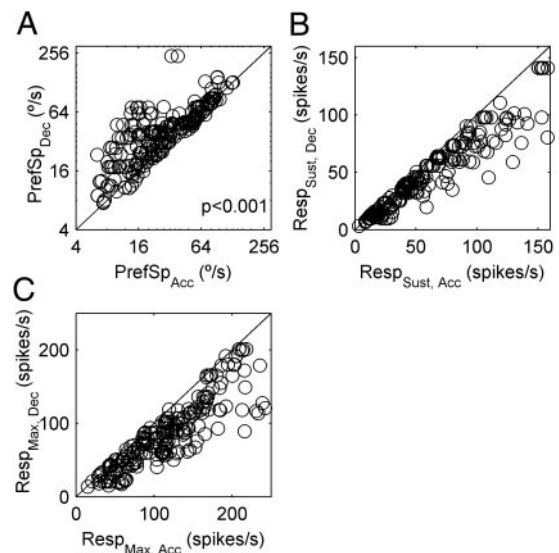


FIG. 13. Model outputs for the population of cells. *A*: preferred speeds inferred from the model responses to acceleration and deceleration. Comparison of sustained (*B*) and maximum (*C*) responses evoked by periods of acceleration and deceleration.

creasing with increasing speed. This speed dependency could cause “compression” of the responses to acceleration because the long-latency responses to low speeds may overlap with the shorter-latency responses to higher speeds. Conversely, response “expansion” may be observed in deceleration responses. Response compression and expansion should lead to higher peak firing rates during acceleration than during deceleration, as we observed (Fig. 5). We incorporated speed-dependent latencies into the model in two ways. First, we used an exponential relationship between speed and latency for each cell, so that latency declined with increasing speed. Second, we used a piecewise-linear fit to the speed-latency curve, with latency declining linearly with increasing speed to a plateau latency for all speeds greater than a threshold value. Using the coefficient of determination between the model output and the actual neuron response, there was no significant improvement in the quality of fits to the acceleration or deceleration periods across the population when the effects of latency were incorporated into the model ($P > 0.1$, two-sample *t*-test).

Comparing model and physiological outputs

To relate the behavior of the model across its population of cells with the data from real MT neurons, we analyzed the model outputs in the same way as for the real cells. Qualitatively the population of modeled and real cells had similar properties. First, preferred speeds indicated by modeled responses to deceleration were higher than those indicated by acceleration (Fig. 13*A*), which is consistent with the findings from MT (Fig. 6*C*). Second, maximum and sustained responses evoked by accelerations were also greater than those evoked by decelerations of the same rate (Fig. 13, *B* and *C*), corresponding with findings from MT (Fig. 5, *A* and *B*).

A population model for reconstructing stimulus speed and acceleration

We have shown that the responses of individual neurons do not explicitly code stimulus acceleration; however, we wanted

to determine to what extent the population response of MT neurons could be used to accurately estimate both stimulus speed and acceleration. Using the physiological data compiled from cells in this study, we built a population-vector-based model that collated the responses from a subpopulation of 41 MT neurons for which we had full speed-tuning data and acceleration responses. Each neuron was described by skewed-Gaussian fits to its transient and sustained speed tuning and its adaptation rate. A neuron's speed-tuning curves were normalized relative to its maximum firing rate, given by the transient response to its preferred speed. From this, each cell's response to a given time-varying stimulus was calculated, as shown previously in Fig. 10. A cell's response at each point in time represents a "vote" for its preferred speed, with the strength of the vote given by the normalized firing rate. A population response estimating the current stimulus speed is calculated by pooling the weighted response of all cells at each point in time

$$S_{\text{Est}}(t) = \frac{\sum v_i S_{\text{Pref},i} \times R_i(t)}{\varepsilon + \sum v_i R_i(t)}$$

where $S_{\text{Est}}(t)$ is the population-based estimate of the speed at time t , $S_{\text{Pref},i}$ is the preferred speed of the i th cell, $R_i(t)$ is the response of the i th cell at time t , and ε is a small positive value that prevents spurious values when $R_i(t) = 0$ for all cells.

Two thresholds were applied to this model. First, a response threshold was used such that a cell's vote was ignored if its response was $<1\%$ of its maximum firing rate. This reduces the sensitivity of the model to noise in the fitted speed-tuning curves. Second, a speed threshold was introduced such that no cells responded to speeds $<3.6^\circ/\text{s}$. This represents half the minimum preferred speed, $\min(S_{\text{Pref},i})$, of all cells in our population. This thresholding was necessary because population-vector-based models cannot correctly respond to stimuli outside the range of preferred speeds for the cell population. If other cells with lower preferred speeds were introduced, the model's ability to accurately reconstruct low stimulus speeds would be substantially improved. Similarly, the population model cannot accurately estimate stimulus speeds greater than the highest preferred speed, $\max(S_{\text{Pref},i})$, and thus in our simulations we restricted stimulus speed to be $<120^\circ/\text{s}$.

Stimulus acceleration can be estimated by differentiating the speed estimate $S_{\text{Est}}(t)$. Differentiation was implemented in a biologically plausible manner by passing the speed estimate through two pathways with different low-pass filters (Ibbotson and Clifford 2001). The filters were first-order Butterworth filters, with exponential impulse responses with time constants of 1.3 and 63 ms. The pathway with a longer time constant implements a substantial delay, and thus subtraction of the two filter outputs yields an unscaled approximation of the derivative of the speed estimate

$$A_{\text{Est}}(t) = F_{\tau_1}[S_{\text{Est}}(t)] - F_{\tau_2}[S_{\text{Est}}(t)]$$

where F_{τ_1} and F_{τ_2} are the two low-pass filters. The filter time constants were chosen to maximize the difference between responses to different acceleration rates.

Figure 14 shows the structure and processing performed by various stages of the population model. Three input speed profiles are shown (Fig. 14A), constituting 1 s of acceleration and deceleration at 40, 80, and $120^\circ/\text{s}^2$. The responses of four MT neurons to the input speed profiles are shown. The cells are ordered from left to right in order of increasing preferred

speed. Importantly, apart from the cell on the right, the responses do not systematically increase with increasing stimulus acceleration (and therefore peak speed). However, the rightmost cell has a negligible response to the speeds in the lowest acceleration profile. This means that without knowing an individual cell's speed tuning, it is impossible to estimate either relative or absolute speeds. The outputs of the population estimate of speed $S_{\text{Est}}(t)$ are shown in Fig. 14B for each of the three input accelerations. Because of the adaptation inherent in the single-cell responses and the constant weighting factors $S_{\text{Pref},i}$ for each cell, $S_{\text{Est}}(t)$ does not precisely match the actual stimulus speed. However, what is important is that there is a monotonic relationship between actual and estimated speed, meaning that different input speeds are distinguished by the model. This allows accurate judgments of relative speed, even if absolute speed cannot be judged.

The output of the ideal observer is passed through the differentiator, yielding the three estimates of stimulus acceleration $A_{\text{Est}}(t)$ shown in Fig. 14C. Ideally, these acceleration estimates would be square-wave pulses of different amplitudes, reflecting the constant acceleration periods in each input stimulus. Although the actual estimates are not square waves, different accelerations clearly evoked different amplitude responses. Importantly, estimates show responses of opposite sign during acceleration and deceleration periods, with graded response amplitudes for different acceleration or deceleration rates. Further, the acceleration estimates are most sensitive during the initial part of an acceleration period but sensitivity emerges more slowly for decelerating stimuli. In this case, sensitivity arises from the differential amplitudes: a larger separation in amplitudes between the responses to different acceleration rates gives greater sensitivity. This separation grows rapidly after acceleration onset, but takes longer to appear after deceleration onset (Fig. 14C). Finally, acceleration estimates do not emerge until ≥ 50 ms after speed estimates are first evident. This long latency reflects the time constants of the low-pass filters used to implement the delay in the differentiator.

DISCUSSION

Acceleration sensitivity influences the initiation and maintenance of pursuit eye movements and may assist in the correct perception of visual motion. The work presented here is the first investigation of acceleration sensitivity in area MT of awake animals. We studied the responses of individual neurons to steps and ramps in stimulus speed, the latter constituting constant acceleration or deceleration. Even though we found no strong evidence for acceleration sensitivity in individual neurons, responses to acceleration cannot be predicted entirely from the responses to constant speeds, suggesting that speed change has some influence on responsiveness. We show that neuronal responses to acceleration are much better predicted by a model combining a cell's speed tuning and adaptation. We show that relative stimulus speed and acceleration can be extracted from the responses of a population of MT neurons.

Acceleration tuning is not found in MT

We found little evidence for a consistent representation of stimulus acceleration in MT neurons. Whereas all neurons

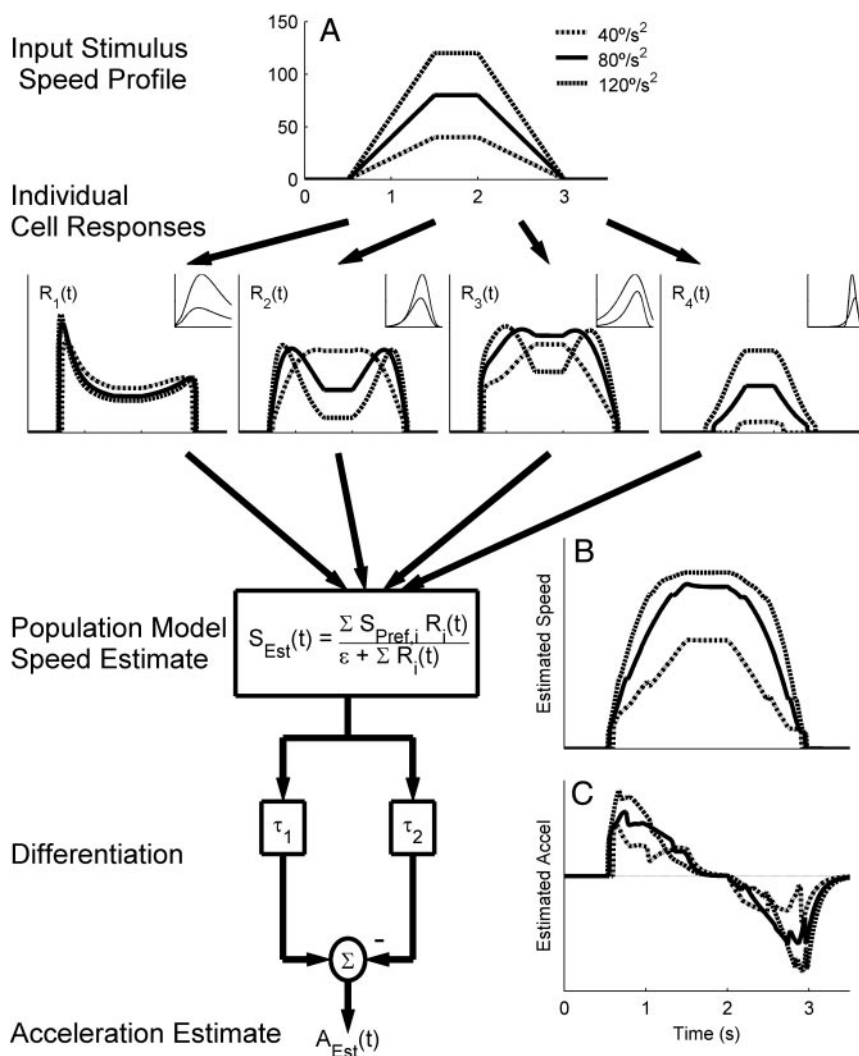


FIG. 14. Population model used to estimate stimulus speed and acceleration. Responses of 4 neurons to 3 stimulus speed profiles (A) are shown. Neuron responses are based on the speed tuning and adaptation of real MT neurons. *Insets:* each cell's transient and sustained speed tuning; preferred speeds using the transient measure were 12, 42, 50, and 95°/s from left to right. Responses of 41 neurons were weighted according to their preferred speed and summed across the population, yielding a population estimate of stimulus speed at all times (B). Line styles in A match the individual response profiles for each model neuron. Differentiation of the speed estimate was approximated by subtracting the outputs of 2 low-pass filters (τ_1 , τ_2), yielding an estimate of stimulus acceleration at all times (C). Note that the estimated speed is a reasonable approximation of the input speed profile in A. Although the estimate of acceleration is relatively poor, it could provide useful information about speed changes.

showed obvious preferred directions and speeds, only 31% showed systematic variation in their maximum responses across the accelerations tested. A similar lack of acceleration sensitivity was reported in anesthetized macaques (Lisberger and Movshon 1999). We chose to expand on the work of Lisberger and Movshon because the speed ramps used in their tests were 128 ms in duration, regardless of the acceleration rate. This means that different acceleration rates present different speed ranges: based on a cell's speed tuning, speed ramps that plateau below the cell's preferred speed should evoke lower responses than ramps that pass through the cell's preferred speed. Thus we used ramps with plateaus of 240°/s, making the tested speed range independent of the acceleration rate.

The results from our neural data can be summarized into three main points. First periods of acceleration generally evoked larger maximum, but similar sustained responses compared with periods of deceleration at the same rate. Second, maximum and sustained responses showed little significant or systematic variation across accelerations and decelerations of different rates. Third, the preferred speeds inferred from responses to deceleration were higher than those predicted from responses to acceleration or steps in stimulus speed.

Neural adaptation could account for the different response rates and preferred speeds associated with acceleration and deceleration. The responses of neurons in area MT show adaptation, typically evident as reduced responsiveness after periods of elevated firing (Kohn and Movshon 2003, 2004; van Wezel and Britten 2002). For a constant speed stimulus, adaptation is evident as a decline in firing rate over time, giving rise to the transient and sustained responses used here to characterize speed tuning. Thus adaptation would be expected to generate smaller responses to deceleration after a period of acceleration, as was usually the case.

It is difficult to determine whether the difference in the timing and amplitude of responses to acceleration and deceleration is the result of adaptation or inherent physiological differences in processing positive and negative speed gradients. However, this is not an important distinction because, practically, real-world deceleration must be preceded by a period of acceleration. Thus if the eyes remain stationary while viewing motion, responses to deceleration are always affected by prior motion. Although a saccade may suddenly bring a neuron's receptive field onto an image region containing deceleration, this neuron will still have experienced prior motion during the saccade (Price et al. 2005). We have demonstrated

that the responses to acceleration are significantly reduced after adaptation with constant speed motion. Further, incorporating adaptation into our model allows the prediction of the responses to both acceleration and deceleration. This demonstrates that adaptation is a fundamental aspect of MT neuron responses to constant and changing motion.

The influence of latency

An alternative explanation for the different responses to acceleration and deceleration is the speed dependency of latencies, which are significantly increased at lower speeds (Lagae et al. 1994; Lisberger and Movshon 1999). This could cause response “compression” during acceleration because long-latency responses to low speeds may overlap with shorter-latency responses to higher speeds. Conversely, response “expansion” may occur in deceleration responses, spreading the responses out over a longer time period. This compression and expansion could lead to higher peak firing rates during acceleration than during deceleration.

We found that the major changes in latency occurred only at speeds $<20^\circ/\text{s}$. Thus speed-dependent variations in latency are likely to affect only the responses to low accelerations. For example, with an acceleration of $960^\circ/\text{s}^2$, speeds $<20^\circ/\text{s}$ are presented for <20 ms. Further, we found that the average difference in time between peak responses to acceleration and deceleration at $240^\circ/\text{s}^2$ was 150 ms. This is far greater than the typical response latencies of 40–80 ms, suggesting that response compression and expansion are unlikely to solely account for the differences in inferred preferred speed.

We used the latency of responses to a cell’s preferred step in speed to infer a preferred speed from the time when responses to a speed ramp peaked. It could be argued that this latency is not appropriate because speed-dependent variations in latency can be as much as 40 ms. For a speed ramp of $240^\circ/\text{s}^2$, this could result in an error in the preferred speed estimate of $\leq 9.6^\circ/\text{s}$. Although this is large relative to the median preferred speed of the population, which was $42^\circ/\text{s}$ (calculated from the sustained response to speed steps), it represents the extreme end of the distribution. Importantly, speed-dependent latency variations are most prominent for speeds $<20^\circ/\text{s}$ but for a ramp rate of $240^\circ/\text{s}^2$ these speeds are presented for only 8.3 ms. Thus for this ramp rate, a more realistic latency error of ≤ 10 ms could be considered, resulting in an error of $<2.4^\circ/\text{s}$ in the estimate of preferred speed. This is insignificant compared with the preferred speeds of most cells.

Single-cell modeling

A neuron’s transient and sustained speed-tuning curves measured using speed steps did not typically capture its responses to speed ramps. By combining the neuron’s speed tuning with adaptation, we were better able to predict the temporal profile of responses to speed ramps and the general response properties observed across the population of cells. As seen in the neuronal data, the model gave larger responses to acceleration than to deceleration and had higher preferred speeds inferred from the responses to deceleration than to acceleration. This suggests that the responses of a neuron to speed ramps are largely explicable in terms of its speed tuning and adaptation. Further, incorporating speed-dependent response latencies did

not improve the power of the model, probably because the variability in latency is mostly evident at low speeds, which were presented for only short durations during our accelerating stimuli.

Although we have attributed the difference in responses evoked by acceleration and deceleration predominantly to adaptation, our experiments do not indicate the mechanisms or locus of this adaptation. However, slow adaptation in MT neurons is most likely related to contrast adaptation and inherited from afferent signals (Kohn and Movshon 2003). The demonstration of adaptation in previous studies of area MT (Kohn and Movshon 2003; Petersen et al. 1985; van Wezel and Britten 2002) and the success of our adapting model in predicting the responses of individual neurons to sustained motion stimuli demonstrate that adaptation is an inherent aspect of neuronal motion analysis. Thus adaptation must be taken into account at the neuronal level, when considering a neuron’s response to changing stimuli, and at the population level, when considering the perception of sustained and changing motion stimuli.

Population modeling to recover acceleration

Lisberger and Movshon (1999) previously suggested that stimulus acceleration may be explicitly resolved from the population response of area MT. However, their model is limited in that accelerations or decelerations from nonzero speeds produce unpredictable interactions between transient and sustained responses; thus for example, their model is unable to distinguish a range of decelerations.

Our population model was able to reliably estimate relative stimulus speed. With the application of an appropriate nonlinear, but continuous and monotonic transform, it would be possible to accurately judge absolute speed. The model also provides acceleration estimates that are of opposite sign for acceleration and deceleration and are graded in amplitude for different acceleration rates. The gradations in estimated acceleration are not as clear as those in the estimated speed profiles, suggesting that the model is better suited to estimating speed. The population model is most sensitive during the early phase of responses to acceleration, but takes much longer for similar sensitivity to arise in response to deceleration. These properties mimic many perceptual findings on acceleration sensitivity, as discussed in the following text. Differentiation of the population speed estimate to obtain an acceleration estimate requires a delayed representation of stimulus speed. Physiologically, filtering may arise through neuronal networks involving self-excitation or mutual inhibition, or at the synaptic level as a result of synaptic depression (Chance et al. 1998; Maex and Orban 1992).

Implications for locus of acceleration sensitivity

It is not clear how human perceptual sensitivity to acceleration is generated. It could arise by population pooling of the responses of neurons with different acceleration tunings in the same way speed perception is thought to arise by pooling the responses of many neurons with different speed tuning. Alternatively, acceleration sensitivity could be generated by assessing changes over time in the population code used to extract stimulus speed, as was incorporated into our population model.

Perceptually, our speed sensitivity is better than our acceleration sensitivity. Psychophysical studies have shown that humans are far better at detecting differences in speed between two targets than they are at detecting stepped or gradual changes in speed (McKee 1981; Schmerler 1976; Snowden and Braddick 1991; Werkhoven et al. 1992). This supports the suggestion that the detection of velocity modulations is not directly based on an acceleration signal, but is generated from the velocity signal (Werkhoven et al. 1992). Further, accurate speed discrimination and acceleration detection require integration times of around 100 ms (Snowden and Braddick 1991; Werkhoven et al. 1992), supporting the extraction of acceleration information from a speed code. Our model shows that reliable estimates of relative stimulus speed can be extracted from the responses of a population of real MT neurons, but that the representation of acceleration is weaker. This appears to fit with real behavioral observations of human perception.

Individual neurons in area MT are sensitive to motion direction and speed and are known to underlie the accurate perception of direction and speed. Despite individual neurons in area MT not being sensitive to motion acceleration and the weak psychophysical evidence for acceleration sensitivity in humans, the speed sensitivity of neurons in area MT may be used to generate acceleration sensitivity for other purposes. Together with the adjacent medial superior temporal area (MST), MT projects directly to the pretectum and DLPN (Ibbotson and Dreher 2005), which contain neurons with a spectrum of sensitivity to both retinal image speed and acceleration (Cao et al. 2004; Das et al. 2001; Ono et al. 2005). Areas MT and MST also project to the frontal eye fields, which subsequently project to NRTP, another pontine area with neurons influenced by retinal image acceleration (Ono et al. 2005). Thus the motion processing performed in area MT is a key input to different components of the cortico-ponto-cerebellar pathway responsible for the generation of smooth pursuit eye movements.

A next step is to measure responses to speed steps and ramps in brain stem regions associated with eye movement control and higher level cortical areas involved in perception. Comparing these responses with the outputs from MT neurons and the model cascade presented here should make it possible to find the site at which retinal acceleration is extracted for use in both eye movement control and perception.

ACKNOWLEDGMENTS

We thank Drs. Valahb E. Das and Nathan A. Crowder and T. Broznya for assistance with data collection and invaluable discussion.

GRANTS

This work was supported by an International Linkage Grant LX0349251 from the Australian Research Council, grants from the Sangora Educational Foundation, and National Institutes of Health Grants EY-06069 and RR-0165.

REFERENCES

- Bair W and O'Keefe LP.** The influence of fixational eye movements on the response of neurons in area MT of the macaque. *Vis Neurosci* 15: 779–786, 1998.
- Born RT and Bradley DC.** Structure and function of visual area MT. *Annu Rev Neurosci* 28: 157–189, 2005.
- Britten KH, Shadlen MN, Newsome WT, and Movshon JA.** The analysis of visual motion: a comparison of neuronal and psychophysical performance. *J Neurosci* 12: 4745–4765, 1992.
- Cao P, Gu Y, and Wang S-R.** Visual neurons in the pigeon brain encode the acceleration of stimulus motion. *J Neurosci* 24: 7690–7698, 2004.
- Chance FS, Nelson SB, and Abbott LF.** Synaptic depression and the temporal response characteristics of V1 cells. *J Neurosci* 18: 4785–4799, 1998.
- Das VE, Economides JR, Ono S, and Mustari MJ.** Information processing by parafoveal cells in the primate nucleus of the optic tract. *Exp Brain Res* 140: 301–310, 2001.
- Gottsdanker RM.** The ability of human operators to detect acceleration of target motion. *Psychol Bull* 53: 477–488, 1956.
- Ibbotson MR and Clifford CW.** Characterising temporal delay filters in biological motion detectors. *Vision Res* 41: 2311–2323, 2001.
- Ibbotson MR and Dreher B.** Visual functions of the retinorecipient nuclei in the midbrain, pretectum and ventral thalamus of primates. In: *Primate Vision*, edited by Kremers J. Chichester, UK: Wiley, 2005.
- Kohn A and Movshon JA.** Neuronal adaptation to visual motion in area MT of the macaque. *Neuron* 39: 681–691, 2003.
- Kohn A and Movshon JA.** Adaptation changes the direction tuning of macaque MT neurons. *Nat Neurosci* 7: 764–772, 2004.
- Krauzlis RJ and Lisberger SG.** Temporal properties of visual motion signals for the initiation of smooth pursuit eye movements in monkeys. *J Neurophysiol* 72: 150–162, 1994.
- Lagae L, Maes H, Raiguel S, Xiao DK, and Orban GA.** Responses of macaque STS neurons to optic flow components: a comparison of areas MT and MST. *J Neurophysiol* 71: 1597–1626, 1994.
- Lisberger SG, Morris EJ, and Tychsen L.** Visual motion processing and sensory-motor integration for smooth pursuit eye movements. *Annu Rev Neurosci* 10: 97–129, 1987.
- Lisberger SG and Movshon JA.** Visual motion analysis for pursuit eye movements in area MT of macaque monkeys. *J Neurosci* 19: 2224–2246, 1999.
- Maex R and Orban GA.** A model circuit for cortical temporal low-pass filtering. *Neural Comput* 4: 932–945, 1992.
- Maunsell JH and Van Essen DC.** Functional properties of neurons in middle temporal visual area of the macaque monkey. I. Selectivity for stimulus direction, speed, and orientation. *J Neurophysiol* 49: 1127–1147, 1983.
- McKee SP.** A local mechanism for differential velocity detection. *Vision Res* 21: 491–500, 1981.
- Nichols MJ and Newsome WT.** Middle temporal visual area microstimulation influences veridical judgments of motion direction. *J Neurosci* 22: 9530–9540, 2002.
- Ono S, Das VE, Economides JR, and Mustari MJ.** Modeling of smooth pursuit-related neuronal responses in the DLPN and NRTP of rhesus macaque. *J Neurophysiol* 93: 108–116, 2005.
- Petersen SE, Baker JF, and Allman JM.** Direction-specific adaptation in area MT of the owl monkey. *Brain Res* 346: 146–150, 1985.
- Pola J, Wyatt HJ, and Lustgarten M.** Visual fixation of a target and suppression of optokinetic nystagmus: effects of varying target feedback. *Vision Res* 35: 1079–1087, 1995.
- Price NS, Ibbotson MR, Ono S, and Mustari MJ.** Rapid processing of retinal slip during saccades in macaque area MT. *J Neurophysiol* 94: 235–246, 2005.
- Raiguel SE, Xiao DK, Marcar VL, and Orban GA.** Response latency of macaque area MT/V5 neurons and its relationship to stimulus parameters. *J Neurophysiol* 82: 1944–1956, 1999.
- Schmerler J.** The visual perception of accelerated motion. *Perception* 5: 167–185, 1976.
- Snowden RJ and Braddick OJ.** The temporal integration and resolution of velocity signals. *Vision Res* 31: 907–914, 1991.
- Stone M.** Cross-validator choice and assessment of statistical predictions. *J R Stat Soc B* 36: 111–147, 1974.
- Suzuki DA, Yamada T, and Yee RD.** Smooth-pursuit eye-movement-related neuronal activity in macaque nucleus reticularis tegmenti pontis. *J Neurophysiol* 89: 2146–2158, 2003.
- van Wezel RJ, and Britten KH.** Motion adaptation in area MT. *J Neurophysiol* 88: 3469–3476, 2002.
- Watamaniuk SNJ and Heinen SJ.** Perceptual and oculomotor evidence of limitations on processing accelerating motion. *J Vision* 3: 698–709, 2003.
- Werkhoven P, Snippe HP, and Toet A.** Visual processing of optic acceleration. *Vision Res* 32: 2313–2329, 1992.